POLITECNICO DI TORINO
Repository ISTITUZIONALE

INVESTIGATION OF REYNOLDS STRESSES PRIOR TO VORTEX BREAKDOWN ON A TRIPLE-DELTA WING AT TRANSONIC CONDITION

Original
INVESTIGATION OF REYNOLDS STRESSES PRIOR TO VORTEX BREAKDOWN ON A TRIPLE-DELTA WING AT TRANSONIC CONDITION / Di Fabbio, T., Tangermann, E., Klein, M.. - (2022). (12th International Symposium on Turbulence and Shear Flow Phenomena (TSFP 2022) Osaka (JPN) July 19-22, 2022).

Availability:
This version is available at: 11583/3012816 since: 2026-07-08T08:11:03Z

Publisher:
Symposia on Turbulence and Shear Flow Phenomena (TSFP)

Published
DOI:

Terms of use:

This article is made available under terms and conditions as specified in the corresponding bibliographic description in the repository

Publisher copyright

(Article begins on next page)

10 September 2026

12th International Symposium on Turbulence and Shear Flow Phenomena (TSFP12)
Osaka, Japan (Online), July 19-22, 2022

INVESTIGATION OF REYNOLDS STRESSES PRIOR TO VORTEX BREAKDOWN ON A TRIPLE-DELTA WING AT TRANSONIC CONDITION

Tony Di Fabbio, Eike Tangermann and Markus Klein
Department of Aerospace Engineering
University of the Bundeswehr Munich
85577 Neubiberg, Germany
tony.difabbio@unibw.de

ABSTRACT

The behavior of leading-edge vortices on a triple-delta wing configuration has been analysed numerically at a side slip condition. The flow is transonic, therefore several shock waves appear over the fuselage with multiple vortex-shock interactions occurring. The paper focuses on the investigation of the Reynolds stress tensor with a detailed analysis of individual components and their relevance for the prediction of the flow features. Three different approaches of turbulence treatment and of constitutive relation have been compared in order to understand the correlation between Reynolds stress field further upstream and the consecutive appearance of vortex breakdown on the windward wing. The Quadratic Constitutive Relation appears in the end a promising approach in order to mitigate the deficiencies of the linear Boussinesq assumption and to predict the flow physics over such configuration with a better accuracy.

INTRODUCTION

Solving the Reynolds averaged Navier-Stokes equations employing one-equation eddy viscosity turbulence models remains the most widely used approach for the prediction of turbulent flows. The eddy-viscosity turbulence models, commonly used to close the RANS equations, are linear models. These models derived from the Boussinesq hypothesis appear to lack capability for prediction of vortical flows. A more realistic effective-viscosity formulation has been proposed by Pope (1975). Its advantage over the isotropic-viscosity hypotheses is that the whole velocity-gradient tensor affects the predicted Reynolds stresses. Two notable consequences of this are that the Reynolds-stress tensor is realistically modelled and the influence of streamline curvature on the Reynolds stresses is incorporated. The failure of isotropic viscosity hypotheses to provide correct predictions in many flow situations either is due to inapplicability of an effective-viscosity approach or to inadequacy of the isotropic-viscosity hypotheses. To remedy some of the shortcomings of the linear eddy-viscosity models, the Quadratic Constitutive Relation (QCR) for eddy viscosity has been proposed by Spalart (2000). QCR uses a nonlinear turbulent stress/strain equation, in contrast to the most commonly used linear Boussinesq relation. Therefore, a key driver is the QCR's ability to modify the incorrect behavior of the Reynolds normal stresses trying to take its anisotropy property into account.

The vortex dominated flow around a triple-delta wing ADS-NA2-W1 as described by Hövelmann *et al.* (2020) has been analysed in the current work. The simulations have been performed employing the DLR TAU-Code (Gerhold (2005)) at transonic conditions with $Ma = 0.85$, $Re = 12.53 \cdot 10^6$ for $\alpha = 20°$ and $\beta = 5°$. The results from three different simulations featuring different turbulence model approaches are presented. Results from URANS based on the linear Boussinesq assumption (LBA), the QCR.2020 nonlinear model version of Spalart-Allmaras (QCR) and hybrid RANS/LES (IDDES) are discussed. The SAneg-based IDDES model is applied in the scale-resolving computations, whereas the Spalart-Allmaras One-Equation Model with corrections for negative turbulent viscosity and rotation/curvature correction (SA-negRC) is employed to close the URANS equations within the QCR and LBA approaches.

Since the flow separation, which forms the initial stage of vortex formation, is fixed by the sharp leading edge, the main challenge within the simulation is to correctly produce formation and further development of the vortical flow system along the wing surface, which is primarily affected by the treatment of turbulence in terms of modeling or resolving turbulent eddies. The IDDES serves as a reference, providing the highest affordable fidelity of flow field prediction. The LBA URANS model, even without the necessity to predict the flow separation, fails to produce several features (including vortex breakdown) of the flow field correctly, as it has been already shown in previous work by the authors (Di Fabbio *et al.*, 2022*a*,*b*). Finally, the QCR.2020 nonlinear model version of Spalart-Allmaras is able to capture the vortex breakdown over the windward wing resulting in a clear improvement in the predicted aerodynamic coefficients.

The present work provides insight to the understanding of the relationship between vortex breakdown and Reynolds stresses. When used in conjunction with the SA turbulence model with rotation/curvature correction, the QCR equation improves the Reynolds stress predictions as will be shown by comparison with IDDES results. This improvement is significant in the observed case, though it is noteworthy, that the momentum equation incorporates the divergence of the Reynolds stresses. Therefore, the gradients of the Reynolds stresses impact the stress-induced vortex breakdown and capturing their absolute levels typically is less significant as it has been discussed by Rumsey *et al.* (2020).

TURBULENCE MODEL

The SAneg-IDDES model according to Spalart *et al.* (1997) and Shur *et al.* (2008) is based on the following trans-

port equation for the modified eddy viscosity

$$\frac{\partial}{\partial t}(\rho\tilde{\nu}) + \vec{u}\cdot\vec{\nabla}(\rho\tilde{\nu}) = \vec{\nabla}\cdot\left(\frac{\mu+\rho\tilde{\nu}}{\sigma}\vec{\nabla}\tilde{\nu}\right) + \\ + \rho\frac{c_{b2}}{\sigma}(\vec{\nabla}\tilde{\nu})^2 + c_{b1}\rho\tilde{S}\tilde{\nu} - c_{w1}f_w\rho\left(\frac{\tilde{\nu}}{\tilde{d}}\right)^2. \quad (1)$$

In the original SA-model the length scale $d = L_{RANS} = d_w$ (distance to the nearest wall), whereas in the IDDES model d is replaced with $\tilde{d} = L_{IDDES}$, defined as follows

$$\tilde{d} = \tilde{f}_d(1+f_e)d + (1+\tilde{f}_d)C_{DES}\Psi\Delta$$

featuring several fitted functions and coefficients of great complexity which shall not be presented further in this context. Besides, Shur & al. (2000) proposed a streamline curvature correction (SA-RC), which alters the production term with a rotation function, applied in the current work just within the URANS computations as in IDDES the vortices are located in the LES zone.

Finally, the QCR can be applied as an extension to every linear eddy-viscosity model τ_{ij}^L in which the Boussinesq assumption approximates the Reynolds stress tensor as follows

$$\tau_{ij}^L = 2\mu_t\left(S_{ij} - \frac{1}{3}\frac{\partial u_k}{\partial x_k}\delta_{ij}\right) - \frac{2}{3}\rho k\delta_{ij}. \quad (2)$$

The objective is to correct the linear Boussinesq relation by adding quadratic, cubic, or even higher-order terms to obtain a nonlinear relation. In the current work, the QCR.2020 method proposed by Rumsey *et al.* (2020), which is given in Eq. 3, is used in conjunction with the SA-negRC model.

$$\tau_{ij,QCR2020} = \tau_{ij}^L + \\ - C_{cr1}^{\text{“}}\left[O_{ij}\tau_{jk}^L + O_{jk}\tau_{ik}^L\right] - C_{cr2}^{\text{“}}\mu_t\sqrt{2W_{mn}W_{mn}}\delta_{ij} \quad (3)$$

NUMERICAL APPROACH

Unsteady simulations have been performed using the DLR TAU-Code (Gerhold (2005)). An implicit dual-time stepping approach has been selected employing a Backward-Euler/LUSGS implicit smoother. The computation of the fluxes has been performed with a central scheme and the matrix dissipation model has been selected. However, in hybrid RANS/LES the artificial dissipation should be reduced in order to prevent excessive damping of the resolved turbulent structures. A (hybrid) low-dissipation low-dispersion discretization scheme (HLD2) and a vorticity-sensitive sub-grid filter scale, which enhances the development of turbulent structures on anisotropic meshes, have been used (Probst & Reuß (2016)). More details regarding the numerical approach and the time length series of the simulation to collect the statistics variables for the different approaches can be found in previous work (Di Fabbio *et al.*, 2022*b*).

GEOMETRY AND MESH

The ADS-NA2-W1 geometry illustrated in Fig. 1 is a 1:30-scaled version of a generic combat aircraft. It is characterized by a triple-delta wing with three different leading-edge sections. The computational mesh is of unstructured topology with 35 prism layers close to the aircraft surface and tetrahedral cells around. The domain size is 50 times the characteristic length L, which is the fuselage length as illustrated in Fig. 1a. It consists of about 40 million cells. Figure 1b shows the inhomogeneous mesh refinement, in which the cells size varies through the computational domain. The mesh is refined most close to the leading edge, where the generation of inboard and the outboard vortices starts. The cell refinement roughly follows the vortices to capture the strong gradients as well as for the IDDES case the resolved turbulent fluctuations. In previous work (Di Fabbio *et al.*, 2022*b*) the mesh has been validated by a convergence study.

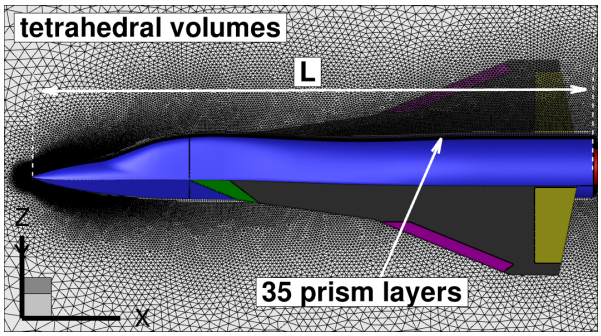

(a) Slice plane $\eta = 0$

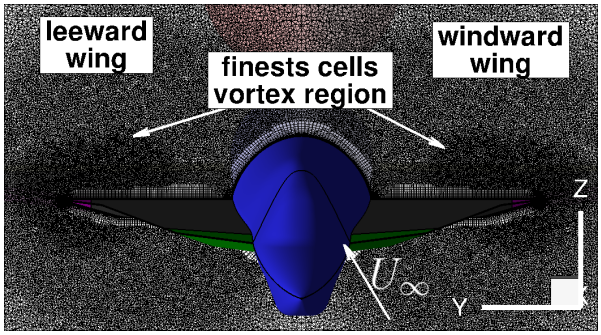

(b) Slice plane $\xi = 0.3$

Figure 1: ADS-NA2-W1 geometry and mesh.

RESULTS

As a primary indicator of result accuracy, the curves of rolling and pitching moment coefficients are shown in Fig. 2. The experimental data according to Hövelmann *et al.* (2020) are plotted in comparison with the CFD results: URANS based on linear Boussinesq assumption (LBA); URANS based on QCR.2020 nonlinear model version of Spalart-Allmaras (QCR); hybrid RANS/LES (IDDES). For a wider overview of the predictions, Fig. 2 also includes aerodynamic coefficients for other angles of attack.

The QCR.2020 method considerably improves the prediction of the aerodynamic coefficients in comparison to the linear SA results especially at $\alpha = 20°$, on which the present work is focused, therefore. The main reason behind the improvement is the prediction of a vortex breakdown above the windward wing which affects the suction footprint over the aircraft as illustrated in Fig. 3. It generates a sudden increase of pressure in the rear part and consequently a drop of local lift. The integral moments of pitching and rolling are very sensitive to such variations of the flow pattern as indicated by the gradients in Fig. 2 which appear at changes of the vortex topology.

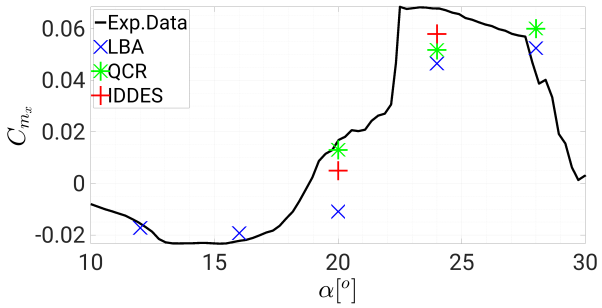

(a) Rolling moment

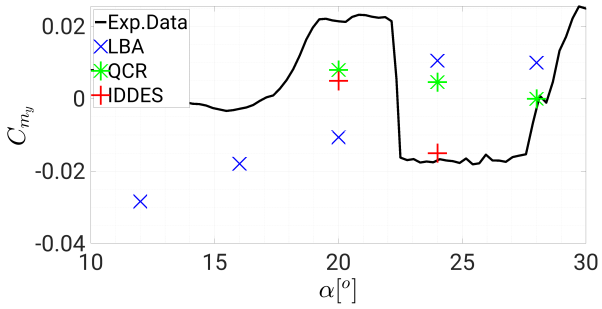

(b) Pitching moment

Figure 2: Aerodynamic coefficients over angle of attack with $Ma = 0.85$, $Re = 12.53 \cdot 10^6$ and $\beta = 5°$.

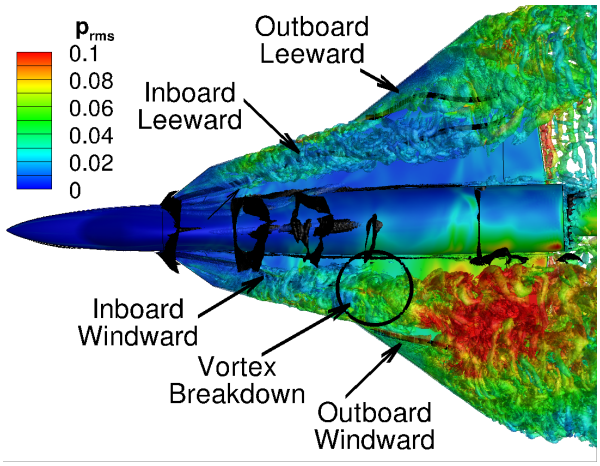

(a) IDDES

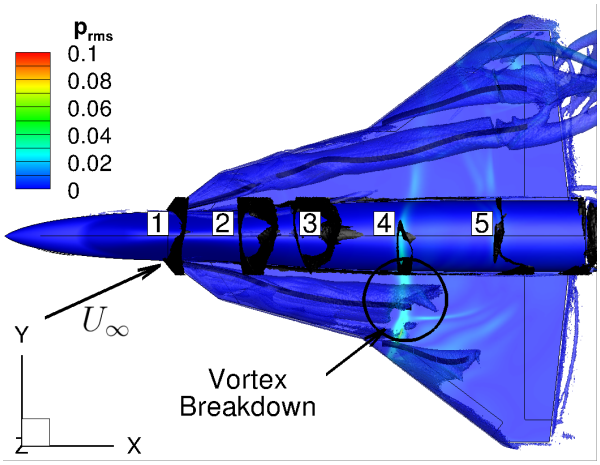

(b) QCR

Figure 3: Rms pressure normalized by free-stream pressure p_{rms}/p_∞ and Q-criterion iso-surface, IDDES and QCR results for $\alpha = 20°$ and $\beta = 5°$. Black: isosurface of $Ma = 1$ and vortex center lines.

Fig. 3a shows the pressure root-mean-square (rms) on a Q-criterion iso-surface and on the aircraft surface from IDDES. p_{rms} has been used to identify the magnitude of the fluctuations. They clearly highlight regions of vortex burst and separated shear-layer. Two well-distinguished vortices are present on the leeward wing and two vortices, closer to each other, are captured on the windward wing breaking down in the rear part. The vortex breakdown appears as an abrupt change in the flow topology where the flow decelerates and diverges. As it has been discussed by Escudier (1988), location and mode of breakdown depend on various parameters such as adverse pressure gradients, type of delta wing planform, angle of attack, sweep angle and interaction with shock waves. As it can be seen in Fig. 3b, the QCR extension also is able to predict the vortex breakdown. The onset location is not fixed, it shows a buffeting behavior. This buffeting is visualized by increased values of p_{rms}. Fig. 3 further shows the iso-surfaces of $Ma = 1$ over the fuselage and highlights the presence of five shock waves (denoted by the numbers in Fig. 3b) between the wing apex and the trailing edge.

The exact shock locations over the fuselage can be seen in Fig. 4, where the ratio p/p_∞ in the symmetry plane $\eta = 0$ is plotted along the surface of the aircraft from the different simulations. The LBA results do not predict the fourth shock wave and consequently the vortex breakdown does not appear. Therefore, the aerodynamic coefficients are predicted wrong, as it has been already discussed before. The p_{rms} plot of the LBA simulation has not been included in the current work as no visible fluctuations have been captured over the wing. The shock waves highlighted in Fig. 4 are caused by the aircraft shape. The fuselage diameter is not constant, as can be seen in Fig. 1 or more precisely in Hövelmann *et al.* (2020). The transonic flow coming from the windward side aligns with the fuselage, follows its shape while being accelerated up to sonic speed and consequently forms a shock wave. The first three shocks in Fig. 3b are caused by this phenomenon. The fifth and final shock is caused by the need for the flow to return to its initial conditions and adjust its pressure field. These shocks due to geometric and boundary conditions are well predicted by all the numerical results. However, it is not possible to give a complete explanation for the presence of the fourth shock. It may be caused by the increase in the sweep angle at the third section of the leading edge. In the following, shock-vortex interaction and Reynolds stresses are analyzed in order to understand the reasons behind the occurrence and prediction of the vortex breakdown on the windward wing.

Fig. 3 also shows indications of the vortex center lines (in black) that have been extracted using an automated criterion. The method considers the maximum of swirl ($S = (\vec{\omega} \cdot \vec{u})/(\rho|\vec{u}|^2)$) in a delimited vortex region in order to determine the vortex core. Fig. 5 shows the extracted vortex center lines from the three different simulation approaches. The simulations predict a similar path. Besides, the vortex breakdown in the IDDES and QCR results can be identified. Fig. 3 and 5 show that in this case of a triple-delta wing configuration with two primary vortices in each side, the inboard vortex is the first one to break down. Since the present study primarily focuses on investigating the Reynolds stresses prior to vortex breakdown, the following analysis considers only the flow physics over the windward wing.

Fig. 6 shows the mean Mach number in the vortex core

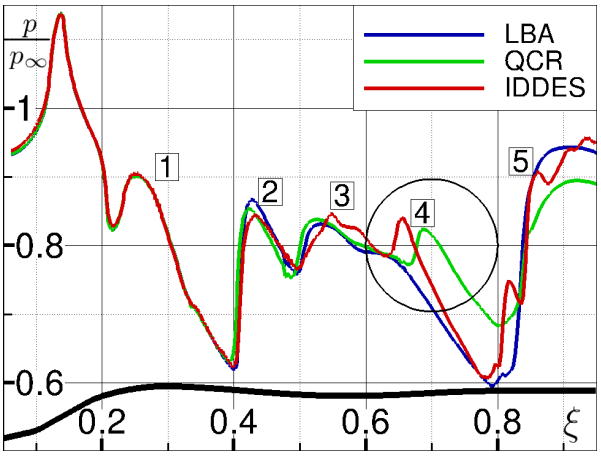

Figure 4: Shock wave locations on the aircraft fuselage. Black line indicates aircraft geometry.

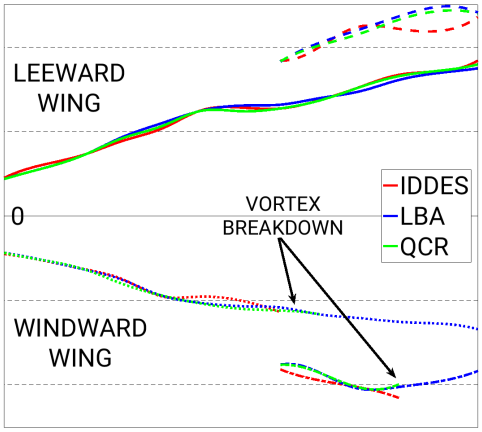

Figure 5: Vortex core line.

lines where the different locations of shock-vortex interaction can be identified. Regarding the IDDES results, the second and third shock in Fig. 4 interact with the inboard windward vortex at around $\xi = 0.4$ and $\xi = 0.5$, respectively, causing a reduction in the streamwise velocity and increasing the vulnerability of the vortex (Delery, 1994). As it can be seen in Fig 6a, the inboard windward vortex breaks at around $\xi = 0.62$ where the interaction with the fourth shock occurs. Without the prediction of shock and vortex breakdown, the LBA produces a rather different Mach number profile. The QCR results are closer to the IDDES high fidelity data and improve the overall prediction of the flow physics. However, the first two shock-vortex interactions are captured slightly upstream at $\xi = 0.4$ and $\xi = 0.45$ and the breakdown at $\xi = 0.65$, which is further downstream over the wing with respect to the IDDES as well as to the experimental results.

Besides, Fig. 6 illustrates the instantaneous Mach number with the dashed lines. The fourth shock wave seems to oscillate in a buffeting way. This oscillation causes a displacement of the interaction plane between the vortex and the shock. This is the primary cause for the unsteadiness of the vortex breakdown which appears in Fig. 3. A clear onset point for the vortex breakdown cannot be determined. The buffeting will have to be discussed in further work dedicated to the unsteady behaviour of such flow physics phenomena.

Fig. 6b shows the mean Mach number in the outboard windward vortex core line. The vortex breakdown location is

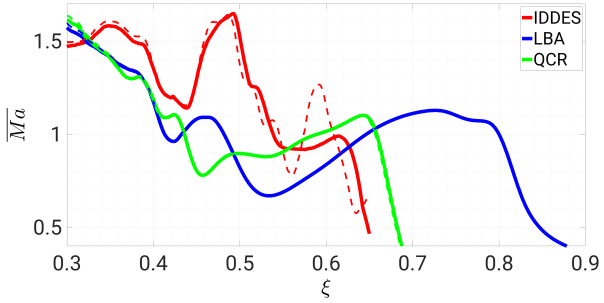

(a) Inboard windward vortex

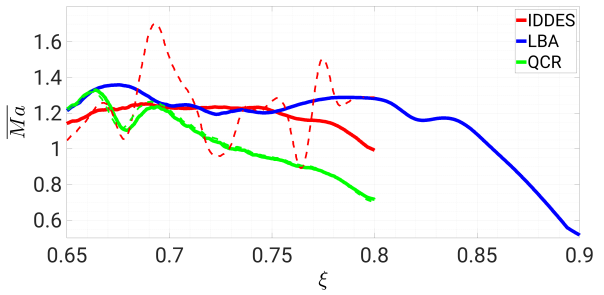

(b) Outboard windward vortex

Figure 6: Numerical evolution of the longitudinal mean Mach number $\overline{Ma}$ in the leading-edge vortex core. Dashed lines indicate instantaneous, solid lines averaged data.

less visible because the flow field is dominated by the inboard vortex burst, as it is evinced by the turbulent fluctuations of the instantaneous Mach number plot. However, a drop of the $\overline{Ma}$ can be seen at around $\xi = 0.66$ from the QCR results and the instantaneous IDDES plot. It indicates the interaction between the inboard vortex breakdown onset as well as shock number 4 and the outboard vortex.

Since the QCR approach significantly improves the results, the anisotrpy of the Reynolds stress is suspected be a driving cause behind the LBA mispredictions. Therefore, the Reynolds stresses are investigated along the vortex core lines in proximity to the vortex breakdown in order to better understand their correlation with this crucial phenomenon. Moreover, the comparison between the different model approaches will help to comprehend the negative effects of the linear Boussinesq assumption. The specific Reynolds stresses have been computed taking into account the resolved and the modeled parts as follows.

$$\tau_{ij}^{tot} = \tau_{ij}^{mod} + \tau_{ij}^{res} \tag{4}$$

where the two contributions have been calculated using the expressions

$$\tau_{ij}^{res} = -\overline{u_i' u_j'} \tag{5}$$

$$\tau_{ij}^{mod} = \tau_{ij}^{L}/\overline{\rho} \quad or \quad \tau_{ij}^{mod} = \tau_{ij,QCR2020}/\overline{\rho} \tag{6}$$

according to the respective approach. Considering the mean flow field, the modeled Reynolds stresses τ_{ij}^{mod} are computed

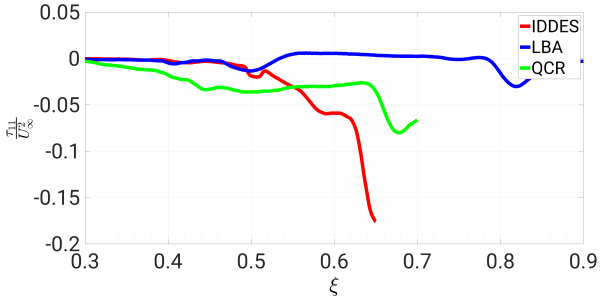

(a) Inboard Windward Vortex

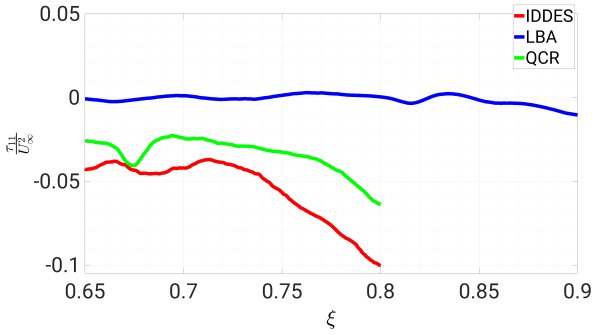

(b) Outboard Windward Vortex

Figure 7: Numerical evolution of the normalized specific Reynolds stress τ_{11}/U_∞ in the leading-edge vortex core.

with the Boussinesq assumption in Eq. 2 or with the QCR.2020 in Eq. 3. On the other hand, the resolved fluctuations have been collected to compute the resolved Reynolds stresses τ_{ij}^{res}.

Fig. 7 shows the normalized specific Reynolds stress τ_{11}/U_∞ along the vortex core lines on the windward side. Velocity fluctuations appear in the leading-edge vortex core even upstream of the breakdown location and it has been demonstrated by Menke & Gursul (1997) that these fluctuations are caused by a random displacement of the vortex core. The averaged Navier Stokes equations only incorporate the divergence of the Reynolds stress tensor. The turbulence effects in the averaged momentum equation can be represented by the body force $f = \nabla \cdot \tau_{ij}$. It means that a negative value of the Reynolds stress tensor gradient produces a negative force that decelerates the flow field over the aircraft. As it can be seen in Fig. 7, the breakdown is characterized by a strong decrease of τ_{11} (the derivative is negative) representing a rapid deceleration of the turbulent flow caused by the aforementioned shock wave. Further, taking a look at the slope of τ_{11} before the inboard vortex breakdown ($0.5 < \xi < 0.6$), the vortex is becoming increasingly vulnerable. The inboard windward vortex is already losing energy and consequently decreasing its axial velocity before the breakdown. This process is not captured by the LBA simulation, where τ_{11} remains almost constant. This phenomenon generates an unsustainable flow condition that leads to the fourth shock over the fuselage and consequently the breakdown. τ_{11} in the outboard vortex core line experiences the effect of the inboard vortex breakdown and the magnitude of the captured fluctuations prior to its breakdown is higher. For this reason, the slope is less pronounced and the breakdown less visible.

Fig. 8 shows components of the normalized Reynolds stress tensor $\tau_{ij} = \overline{u_i' u_j'}/U_\infty^2$ on the windward wing. τ_{ij} represents the intensity of the turbulent fluctuations along the three directions and their covariance. The components of the Reynolds stress tensor have been normalized by free-stream velocity and local mean density. τ_{11} shows the turbulent behavior of the transported turbulent shear-layer. The turbulent motion becomes more intense once the vortex breaks down and the turbulence kinetic energy is then transported downstream. The covariance τ_{12} can be mainly considered to visualize the vortex cores and the region of separated shear-layer close to the leading edge, where its value is negative. τ_{22} indicates that the fluctuations are generated as the flow departs from the leading-edge. It is also the primary origin of the high turbulence kinetic energy in the vortex core. Finally, as it can be seen from the legend scale, τ_{23} is the strongest covariance component and it mainly acts in the shear-layer where the complex process of separation and rolling-up appears.

It is important to highlight how the QCR extension improve the URANS results, even approaching in magnitude the resolved Reynolds stresses from IDDES. The anisotropy of the Reynolds stresses has not been predicted by the LBA which underlines the shortcomings of linear eddy viscosity models applied for vortical flows. In particular, as it can be seen in the τ_{12} plot, QCR allows to model the Reynolds stresses better close to the leading edge which are then involved in the roll-up process feeding the vortex with turbulence kinetic energy. This could explain the higher Mach number in the vortex core seen above and the occurrence of the forth shock which is not predicted by the LBA. However, both the URANS approaches overestimate the prediction of τ_{23}. Consequently, the modeled vortex is stronger, less vulnerable and the probability of vortex breakdown occurrence decreases.

CONCLUSIONS AND OUTLOOKS

Numerical simulations have been performed to analyze the leading-edge vortex behavior on a triple-delta wing configuration in a side slip condition. Results from URANS based on linear Boussinesq assumption, QCR.2020 nonlinear model version of Spalart-Allmaras and hybrid RANS/LES have been compared.

The simulation results show that the application of the Quadratic Constitutive Relation improves the accuracy compared to standard linear eddy-viscosity models not only in terms of integral coefficients of forces and moments but also regarding specific flow features like shocks and vortex breakdown. This observation has been supplemented with a discussion of the Reynolds stress components modeled and resolved by the different methods, respectively. The results underline the shortcomings of linear eddy viscosity models due to the lack of considering the aspects of anisotropy, namely the differences between streamwise, wall-normal, and lateral Reynolds stresses. This affects not only the accuracy of the results but also the resolved flow physics over the wing. The present study serves as a basis and motivation for the development of a modified constitutive relation for specific applications in future work.

REFERENCES

Delery, Jean M. 1994 Aspects of vortex breakdown. *Progress in Aerospace Sciences* **30** (1), 1–59.

Di Fabbio, T., Tangermann, E. & Klein, M. 2022*a* Flow pattern analysis on a delta wing at transonic speed. AIAA SCITECH 2022 Forum, San Diego, CA.

Di Fabbio, T., Tangermann, E. & Klein, M. 2022*b* Investigation of transonic aerodynamics on a triple-delta wing in side slip conditions. *CEAS Aeronautical Journal* .

Escudier, Marcel 1988 Vortex breakdown: Observations

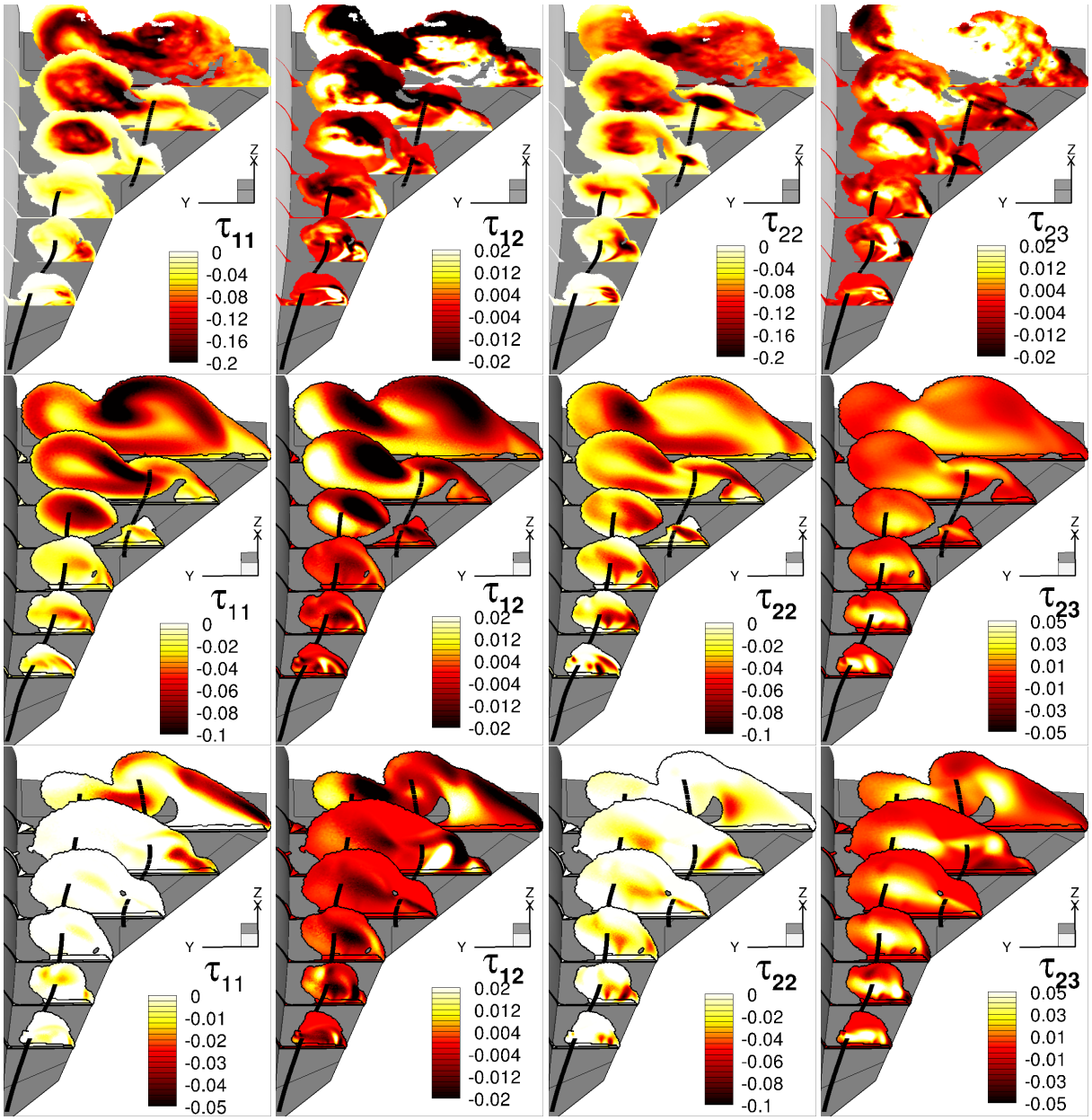

Figure 8: Normalized specific Reynolds stress components, IDDES (top), QCR (middle) and LBA (bottom). Vortex core lines illustrated in black over the aircraft.

and explanations. *Progress in Aerospace Sciences* **25** (2), 189–229.

Gerhold, Thomas 2005 Overview of the hybrid rans code tau. In *MEGAFLOW - Numerical Flow Simulation for Aircraft Design* (ed. Norbert Kroll & Jens K. Fassbender), p. 81–92. Berlin, Heidelberg: Springer Berlin Heidelberg.

Hövelmann, A, Winkler, A, Hitzel, S M, Richter, K & Werner, M 2020 Analysis of vortex flow phenomena on generic delta wing planforms at transonic speeds. In *New Results in Numerical and Experimental Fluid Mechanics XII*, pp. 307–316. Cham: Springer International Publishing.

Menke, Matthew & Gursul, Ismet 1997 Unsteady nature of leading edge vortices. *Physics of Fluids* **9** (10), 2960–2966.

Pope, S. B. 1975 A more general effective-viscosity hypothesis. *Journal of Fluid Mechanics* **72** (2), 331–340.

Probst, A & Reuß, S 2016 Progress in scale-resolving simulations with the dlr-tau code. Deutscher Luft- und Raumfahrtkongress, Braunschweig, Deutschland.

Rumsey, C. L., Carlson, J.-R., Pulliam, T. H. & Spalart, P. R. 2020 Improvements to the quadratic constitutive relation based on nasa juncture flow data. *AIAAJ* **58**.

Shur, M L & al. 2000 Turbulence modeling in rotating and curved channels:assessing the spalart-shur correction. *AIAA Journal* **38** (5).

Shur, Mikhail L., Spalart, Philippe R., Strelets, Mikhail Kh. & Travin, Andrey K. 2008 A hybrid RANS-LES approach with delayed-DES and wall-modelled LES capabilities. *International Journal of Heat and Fluid Flow* **29** (6), 1638–1649.

Spalart, P. R. 2000 Strategies for turbulence modelling and simulations. *International Journal of Heat and Fluid Flow* **21** (3), 252–263.

Spalart, P R, Jou, W H, Strelets, M & Allmaras, S R 1997 Comments on the feasibility of les for wings, and on a hybrid rans/les approach. First AFOSR International Conference on DNS/LES, Ruston, LA.